MULTICONDUCTOR CELL ANALYSIS OF POWER CABLE STEADY STATE

Roberto BENATO, University of Padova, (Italy), roberto.benato@unipd.it

ABSTRACT

The paper deals with the multiconductor analysis of transmission lines namely AC underground cable lines (UGC). A multiconductor matrix procedure based on the use of admittance matrices, which account for the line cells (with earth return currents), different types of sheath bonding, possible multiple circuits, allows predicting the steady-state regime of any cable system. In particular, the method calculates the proportion and behaviour of the phase currents carried by each parallel conductor, the circulating current in the sheath of each cable and the stray current in the earth. A general outline of the multiconductor cell analysis has been thoroughly developed in [1]. Only a brief description of the theoretical procedure will be given in the paper making more room for some examples of application.

KEYWORDS

Underground cables, Multiconductor Matrix Analysis, Extra High Voltage, Short-circuit condition.

INTRODUCTION

The necessity of enforcing the electrical transmission network has become an unavoidable issue to any transmission system operator (TSO). On the other hand, many TSOs have experienced insurmountable difficulties in erecting new overhead lines. Therefore, "underground" technologies as UGC or Gas Insulated Lines (GIL) will play a leading role in the future transmission grids. The possibility of integrating power transmission and other services (i.e. railway and highway transport, bridges, galleries) in the same corridor or in the same "structure" is another fascinating technical challenge favouring underground technologies [2,3]. UGC and GIL are examples of multiconductor systems (phases and sheaths or enclosures) which cannot be studied in detail by means of a simplified single-phase equivalent circuit. The author has already presented a powerful procedure in order to evaluate the transmission operating characteristics of long AC cables [4] and mixed overhead-cable links [5]. The present method, which considers the transmission line in its real asymmetric structure, allows:

- Detecting the exact current sharing between single-core cables and the circulating currents in the sheaths of any number of circuits and with any bonding configuration (cross-bonding, single-point-and solid-bonding);
- Knowing the precise steady-state behaviour of any component of the cable line (e.g. cross-bonding boxes);
- Considering possible phase transpositions;
- Studying the short-circuit regime and the voltages in any line section (consequently the touch-voltages);
- Studying the power loss behaviour along the line;
- Including, for cables installed in a tunnel, the grounding conductors e.g. longitudinal wires or the steel reinforcement of the tunnel itself.

MULTICONDUCTOR MATRIX PROCEDURES: BRIEF DESCRIPTION OF THE METHOD

A single-circuit UGC composed of three single-pole cables is a multiconductor system of *n=6* conductors (*3* phases and 3 sheaths) parallel to themselves and to the ground. If a double-circuit UGC is considered, n=*12* etc. In fig. 1, the conductors can be identified as follows: *1, 2, 3* are the phase conductors and *4, 5, 6* are the metallic sheaths.

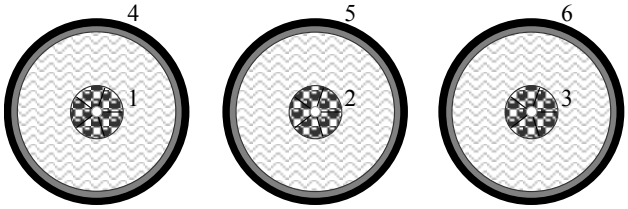

Figure 1: Basic single-pole EHV UGC (flat arrangement)

The line may be represented as a cascade connection of *m* elementary cells of length Δ_ℓ (suitably chosen i.e. ranging between *100* and *300* m), modelled by a lumped PI-circuit (see fig. 2) where the voltage column vectors $\underline{\boldsymbol{u}}_S$, $\underline{\boldsymbol{u}}_R$ and the current column vectors $\underline{\boldsymbol{i}}_S$, $\underline{\boldsymbol{i}}_{SL}$, $\underline{\boldsymbol{i}}_{ST}$, $\underline{\boldsymbol{i}}_R$, $\underline{\boldsymbol{i}}_{RL}$, $\underline{\boldsymbol{i}}_{RT}$ are shown. Being that Δ_ℓ is sufficiently small (neglecting the border effects), it is possible to lump the uniformly distributed shunt admittances at both ends of the cell (transverse blocks T_S and T_R) and to consider separately the longitudinal elements in the block *L* (where $\underline{\boldsymbol{i}}_{RL} \equiv -\underline{\boldsymbol{i}}_{SL}$). Self and mutual longitudinal impedances, which account for the earth return currents, can be obtained by applying the simplified or the complete Carson's theory [6, 7] or Wedepohl's theory [8]. The matrix $\underline{\boldsymbol{Z}}_L$ ($n\times n$) that characterises the longitudinal block *L* can be formed as in *Sect. A*. By considering that

$$\begin{aligned} &\underline{\boldsymbol{u}}_S - \underline{\boldsymbol{u}}_R = \underline{\boldsymbol{Z}}_L\, \underline{\boldsymbol{i}}_{SL} \quad , \\ &\underline{\boldsymbol{i}}_{RL} \equiv -\underline{\boldsymbol{i}}_{SL} \end{aligned} \qquad [1]$$

being $\underline{\boldsymbol{Z}}_L$ non-singular, the following matrix relation yields

$$\begin{bmatrix} \underline{\boldsymbol{i}}_{SL} \\ \underline{\boldsymbol{i}}_{RL} \end{bmatrix} = \begin{bmatrix} \underline{\boldsymbol{Z}}_L^{-1} & -\underline{\boldsymbol{Z}}_L^{-1} \\ -\underline{\boldsymbol{Z}}_L^{-1} & \underline{\boldsymbol{Z}}_L^{-1} \end{bmatrix} \begin{bmatrix} \underline{\boldsymbol{u}}_S \\ \underline{\boldsymbol{u}}_R \end{bmatrix} ; \qquad \underline{\boldsymbol{i}}_{L\Delta} = \underbrace{\underline{\boldsymbol{Y}}_{L\Delta}}_{(2n\times 2n)}\, \underline{\boldsymbol{u}}_\Delta \qquad [2]$$

the vectors of the shunt currents at sending-end $\underline{\boldsymbol{i}}_{ST}$ and at receiving-end $\underline{\boldsymbol{i}}_{RT}$ are

$$\begin{bmatrix} \underline{\boldsymbol{i}}_{ST} \\ \underline{\boldsymbol{i}}_{RT} \end{bmatrix} = \begin{bmatrix} \underline{\boldsymbol{Y}}_{TS} & \\ & \underline{\boldsymbol{Y}}_{TR} \end{bmatrix} \begin{bmatrix} \underline{\boldsymbol{u}}_S \\ \underline{\boldsymbol{u}}_R \end{bmatrix} ; \qquad \underline{\boldsymbol{i}}_{T\Delta} = \underbrace{\underline{\boldsymbol{Y}}_{T\Delta}}_{(2n\times 2n)}\, \underline{\boldsymbol{u}}_\Delta \qquad [3]$$

$\underline{\boldsymbol{Y}}_{TS}$ and $\underline{\boldsymbol{Y}}_{TR}$ ($n\times n$) are defined in *Sect. B*.

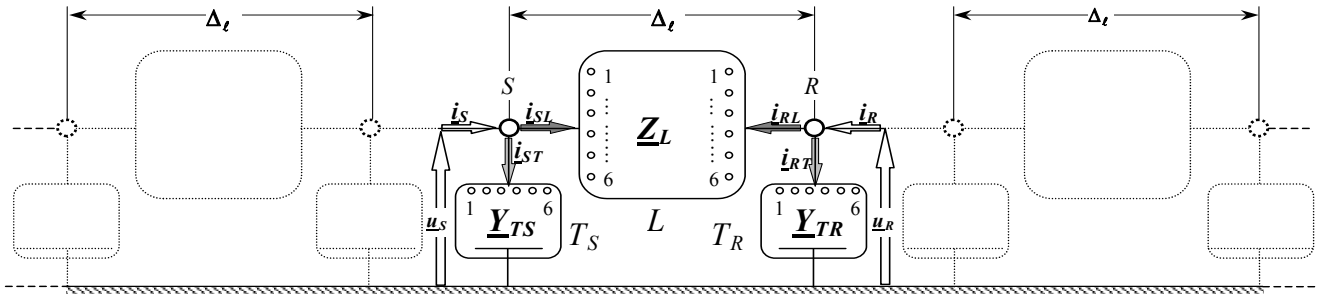

Figure 2: Elementary cell cascade for single-circuit cable line modelling

The superimposition of (2) and (3) yields

$$\begin{bmatrix} \underline{i}_S \\ \underline{i}_R \end{bmatrix} = \underline{Y}_{L\Delta} + \underline{Y}_{T\Delta} \begin{bmatrix} \underline{u}_S \\ \underline{u}_R \end{bmatrix} \qquad [4]$$

$\underline{i}_\Delta$; $\underline{Y}_\Delta$ $(2n \times 2n)$; $\underline{u}_\Delta$

which completely represents the steady-state regime of the elementary cell (of length Δ_ℓ). The cell matrix dimension $\underline{Y}_\Delta$ is $2n \times 2n$.

A. Computation of $\underline{Z}_L$ by means of simplified Carson-Clem's formulae

If $d_{i,j} \leq 0{,}135\ D_{CA}$ (see [7], Vol.II, pag. 154), the self and mutual longitudinal impedances can be obtained by means of the Carson-Clem's formulae (5) and (6):

$$z_{i,i} = r_i + \pi^2 \cdot 10^{-4} \cdot f + j \cdot 4\pi \cdot 10^{-4} \cdot f \cdot ln\left(\frac{2D_{CA}}{d'_i}\right) [\Omega/\text{km}] \qquad [5]$$

$$z_{i,j} = \pi^2 \cdot 10^{-4} \cdot f + j \cdot 4\pi \cdot 10^{-4} \cdot f \cdot ln\left(\frac{D_{CA}}{d_{ij}}\right) \quad [\Omega/\text{km}] \qquad [6]$$

where

r_i = resistance per unit length of conductor i (the skin and proximity effects can be computed by means of IEC 287; Milliken conductors, if enamelled, dramatically reduce them);

$D_{CA} = 660\sqrt{\rho_{soil}/f}$ [m] "Carson's Depth";

f = power frequency, (50, 60 Hz);

ρ_{soil} = electrical resistivity of the soil [Ω·m];

d'_i = 2 GMR [m] (Geometrical Mean Radius); usually in EHV XLPE-cables the conductor is hollow Milliken type; for GMR, see [7], Vol.II, pag. 155;

$d_{i,j}$= mutual distance [m] between conductors i and j (fig. 3 case a).

When the conductors i and j are coaxial, it yields $\underline{z}_{i,j}=\underline{z}_{i,j}=\underline{z}_{j,i}$ where j is the external conductor and i the inner one (see fig. 3 cases b). With regard to the computation of $\underline{Z}_L$ by means of complete Carson's theory and Wedephol's one refer to [1]. However, the use of simplified Carson-Clem's formulae represents a powerful choice at power frequency.

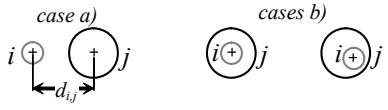

Figure 3: Possible configurations of i and j conductors

B. Computation of $\underline{Y}_{T\Delta}$

The two matrices $\underline{Y}_{TS} = \underline{Y}_{TR}$ can be computed taking into account the shunt capacitive and conductive links. The self and mutual admittances of *half cell* are considered suitably arranging the following two formulae

$$\underline{y}_1 = g_1 + j\omega\, c_1 = \left[\omega \cdot 2\pi \cdot \varepsilon_1 \cdot (tan\delta_1 + j)\right] \Big/ ln\left(\frac{r_2}{r_1}\right) \qquad [7]$$

$$\underline{y}_2 = g_2 + j\omega\, c_2 = \left[\omega \cdot 2\pi \cdot \varepsilon_2 \cdot (tan\delta_2 + j)\right] \Big/ ln\left(\frac{r_4}{r_3}\right) \qquad [8]$$

in which (see fig. 4) g_1 and g_2 represent the leakage conductances across inner and outer insulations, ε_1, ε_2 and $tan\delta_1$, $tan\delta_2$ the corresponding dielectric constants and loss factors respectively. For instance, the admittance matrices $\underline{Y}_{TS}=\underline{Y}_{TR}$ of a single-circuit cable line are given by:

$$\underline{Y}_{TS}=\underline{Y}_{TR}= \cdot \frac{\Delta_\ell}{2}$$

	1	2	3	4	5	6
1	$\underline{y}_1$			$-\underline{y}_1$		
2		$\underline{y}_1$			$-\underline{y}_1$	
3			$\underline{y}_1$			$-\underline{y}_1$
4	$-\underline{y}_1$			$\underline{y}_1+\underline{y}_2$		
5		$-\underline{y}_1$			$\underline{y}_1+\underline{y}_2$	
6			$-\underline{y}_1$			$\underline{y}_1+\underline{y}_2$

When the installation is not completely embedded in the soil, a precise computation of $\underline{y}_2$ is problematic but less important if the sheaths are multi-point earthed. This is the very case of cross-bonding arrangement where the sheaths are earthed at each major section end.

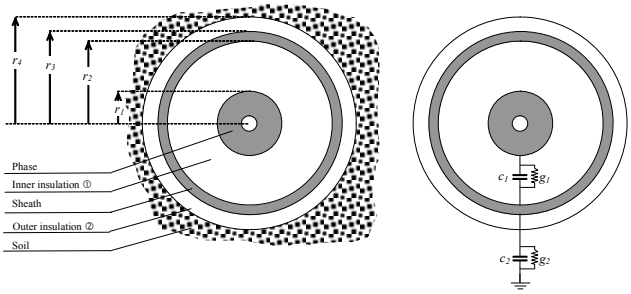

Figure 4: Scheme for the computation of shunt admittances

The steady-state regime of a double-circuit EHV UGC

The structure and assembling of involved matrices will not be shown here for brevity's sake but they are thoroughly shown in [1]. Once $\underline{\underline{Y}}_{\Delta}$ has been computed, it is necessary to achieve the admittance matrix $\underline{\underline{Y}}$ of the whole multiconductor system. The creation of $\underline{\underline{Y}}$ involves all the following matrices: the equivalent supply matrix $\underline{\underline{Y}}_{Aph}$ (3×3) [*1*], the double-circuit sending-end matrix $\underline{\underline{Y}}_S$ [1], the cell matrices $\underline{\underline{Y}}_{\Delta i}$, the bonding matrices $\underline{\underline{Y}}_b$ [1], the double-circuit receiving-end matrix $\underline{\underline{Y}}_R$ [1] and the matrix $\underline{\underline{Y}}_{Load}$ (3×3) [1]. $\underline{\underline{Y}}$ is calculated by using automatic topological procedures that give rise to a partial superposition of matrices. The use of the admittance frame of reference allows introducing easily local modifications of the system structure without reconstructing its entire matrix. An important implication of this fact is the possibility of considering any other lumped shunt component (e.g. reactive compensation devices anywhere along the line including both ends). In fact, they can be represented by their admittance matrices $\underline{\underline{Y}}_{shunt}$ ($n \times n$), which must be superimposed in the right location of the matrix $\underline{\underline{Y}}$ so to give a new "total" matrix $\underline{\underline{Y}}_{TOT}$.
It is worth noting that the matrix approach can consider different kinds of transpositions. Moreover the SPB and SB can be accounted for in these matrices. This procedure can easily consider any number of circuits in parallel or not, any cable arrangement (trefoil, vertical, horizontal etc). Therefore it is completely general and does not need any algebraic manipulation as in the previous contributions [9] or loop current analysis [10, 11]. It is worth remembering that IEC Standard 60287-1-3 [11] is valid only for solid-bonded cables.
Also the short-circuit analysis can be assessed by means of this multiconductor procedures [1].

APPLICATION TO DIRECTLY-BURIED EHV UGC

The proposed multiconductor algorithms are applied to a double-circuit *2500* mm^2 (see fig. 5) copper-conductor UGC whose geometrical and electrical characteristics are reported in tab. 1. The ampacity of tab.1 has been evaluated by means of IEC 287 in case of perfect CB. It is worth noting that the trefoil arrangement can also be suitably studied by this multiconductor matrix analysis even if it cannot evaluate the skin and proximity effects. When these effects can be relevant, a more suitable approach can be adopted [12]. Fig. 6 shows the sheath voltage and current magnitudes when the double-circuit cable line is cross-bonded with 7 major sections (*1,5 km* long). In this case, the CB sections have equal length. In the real installations, it may happen that the CB section lengths are unequal: this multiconductor procedure suits very well also this possibility.

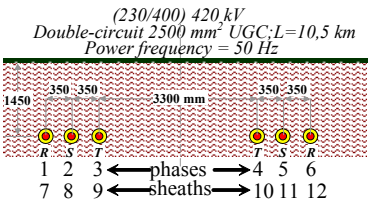

Figure 5: Double-circuit cable line in CB (RST-TSR phase arrangement)

Table 1 Data of 400 kV XLPE UGC

Cross-section		**mm^2**	*2500 Cu*
Diameter on conductor (Milliken)	$2 \cdot r_1$	**mm**	*63,4*
Diameter on XLPE insulation	$2 \cdot r_2$	**mm**	*119,9*
Diameter on metallic sheath	$2 \cdot r_3$	**mm**	*130,1 Al*
Cross-section of sheath		**mm^2**	*≈ 500*
Diameter on PE coating	$2 \cdot r_4$	**mm**	*141,7*
Total mass		**kg/m**	*37*
AC phase resistance at 90°C (50 Hz)	r_{ph}	**mΩ/km**	*10,8*
Inductance	ℓ	**mH/km**	*0,576*
Shunt Leakage (50 Hz) with tanδ=0,0007 (XLPE)	g_1	**nS/km**	*51,5*
Capacitance with ε_r=2,3 (XLPE)	c_1	**μF/km**	*0,234*
Shunt Leakage (50 Hz) with tanδ=0,001 (PE)	g_2	**nS/km**	*470,6*
Capacitance with ε_r=2,3 (PE)	c_2	**μF/km**	*1,5*
Ampacity (cross-bonded, $\rho_{th\text{-}soil}$=1,0 Km/W; θ_{cond}=90°C; $\theta_{ambient}$=20°C)	I_a	**A**	*1788*
Cable drum		**m**	*500*
Cross-bonding major section length		**km**	*1,5*
Route Length	L	**km**	*10,5*
Substation earth resistance	R	**Ω**	*0,1*
Earth resistivity	ρ_{soil}	**Ω·m**	*100*
Cross-bonded box resistance	R_b	**Ω**	*10*
Sheath resistance at 78,2°C (50 Hz)	r_{sh}	**mΩ/km**	*70,0*
Link resistance	r	**mΩ**	*1*

The currents in fig. 6 are capacitive, which cannot be zeroed. Differently, fig. 7 deals with CB without phase transpositions. The use of phase transpositions gives an electrical symmetrization (fig. 6) so that the sheath currents result further reduced from fig. 7 to fig. 6. Therefore, the phase transpositions are unnecessary in case of trefoil arrangement (which has already an intrinsic symmetry). It follows that a cross-bonded UGC with transpositions has lower power losses than one without transpositions: this implies a higher ampacity. In general, the sheath voltage magnitudes along the line, in CB, constitute rather high touch-voltages for operator safety: this is the "price to pay" to considerably reduce the induced currents in the sheaths.

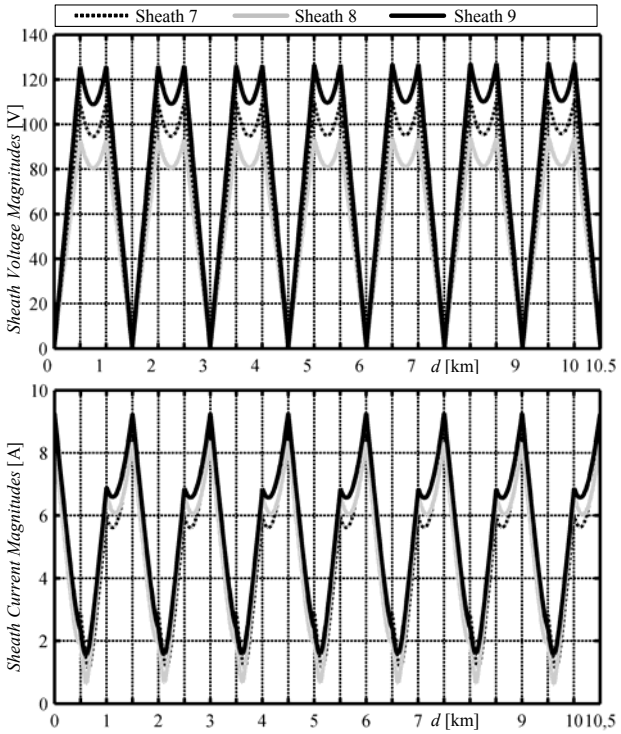

Figure 6: Sheath voltage and current magnitudes along the double-circuit with 7 CB major sections

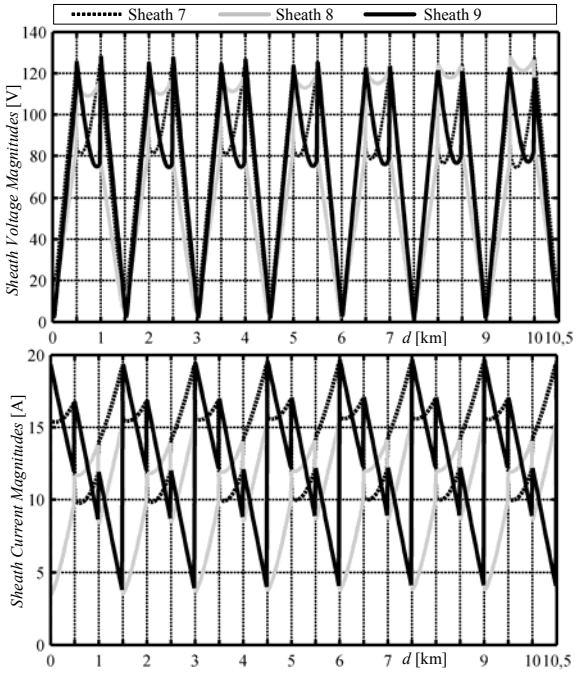

Figure 7: Sheath voltage and current magnitudes along the double-circuit UGC (CB without phase transpositions)

Fig. 6 and fig. 7 show the voltage and current magnitudes of the sheaths belonging to a circuit: the sheaths 10, 11, 12 are overlapped with the sheaths 9, 8 and 7 respectively. If the phase arrangement is RST-RST (often named super bundle configuration), the whole loading is not equally shared between the two circuits. The simulations have been also compared with the *Cable Constants* supporting routine of the ElectroMagnetic Transients Program (EMTP) [13, 14] (here not shown): the multiconductor matrix analysis has demonstrated a greater adaptability to any type of installation (e.g. tunnel installation with its steel reinforcement used as distributed grounding). The stray current in the earth can be easily computed by knowing the current phasors in all the system conductors i.e.

$$\underline{i}_0 = -\sum_{i=1}^{n} \underline{i}_i \,.$$

Fig. 8 shows the steady-state stray current in the earth with CB (with phase transpositions): it is absolutely negligible. This situation changes if CB without phase transpositions is considered. The higher degree of asymmetry implies a higher value of stray current in the earth (about *70* A) as fig. 9 clearly shows.

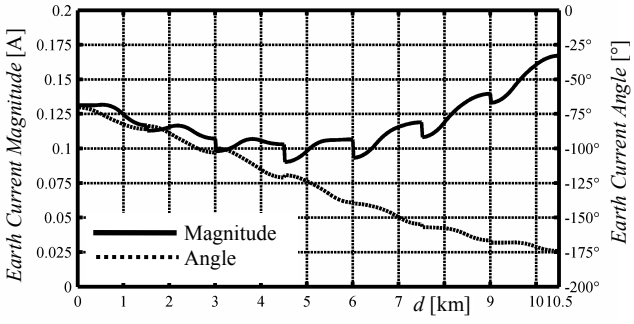

Figure 8: Stray currents in the earth in steady state regime (CB with phase transpositions)

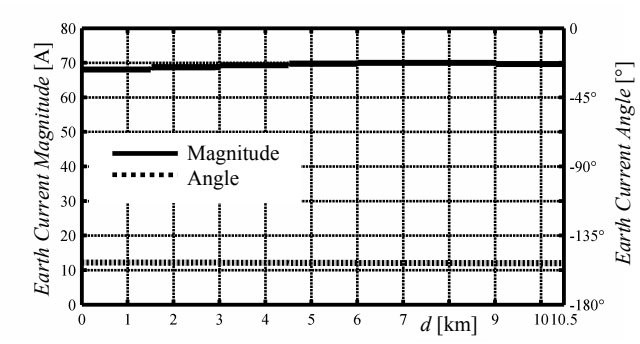

Figure 9: Stray currents in the earth in steady state regime (CB without phase transpositions)

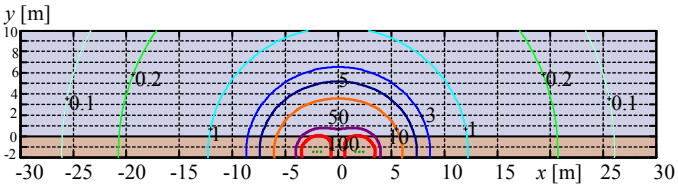

Figure 10: Magnetic induction generated by the UGC double-circuit with I=1788 A

The knowledge of the stray current in the earth is extremely important when the electro-magnetic interferences (EMIs) with parallel metallic systems (where the distances between the group of the inducing conductors and the induced one can be considered as equal) are assessed.
The magnetic induction levels generated by the system (see fig. 10) are low even if with such bulk power transmission (|***S***|=1240 MVA per circuit). This is due to the phase arrangement (RST-TSR often named low-reluctance configuration). Of course, trefoil laying would have considerably lessened the magnetic induction levels but would have also had a fewer ampacity.

SHORT-CIRCUIT ANALYSIS

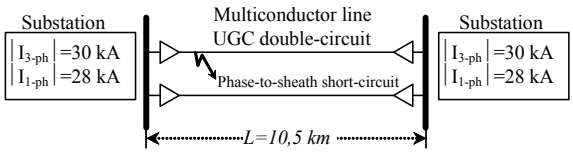

Figure 11: Multiconductor line in short-circuit condition supplied by both end stations

The presence of end substations with equal fault levels (characterized by the three-phase $I_{3\text{-}ph}$ and single-phase $I_{1\text{-}ph}$ subtransient currents as in fig. 11) can be easily accounted for by means of the procedures in [1]. The short-circuit between a phase and the corresponding sheath can be considered by means of a matrix $\boldsymbol{Y_g}$ [1]. The following figures refer to the phase 2-sheath 8 short-circuit at line mid-point (*5,25 km* from both ends). The exact knowledge of the sheath voltages along the cable (see fig. 12 and 13) and in particular on the cross-bonding boxes allows planning the surge arresters (non-linear resistors), which must protect the sheaths from transient overvoltages. The possibility of an accurate calculation depends upon the certainty of data e.g. the earthing resistances R_b, which are unknown until the installation is completed. Notwithstanding these uncertain values can be foreseen in a reasonable range.

Fig. 14 shows the earth current magnitude and angle: it is worth noting that the intermediate grounding points along the line (every *1,5 km*) determine an injection of current in the earth so giving about *250 A*. They can be dangerous for EMIs towards neighbouring parallel metallic systems even if these possible interferences last only the fault clearance time. The earth current can be higher than that in the case of mid-line short-circuit (minimum value). In order to demonstrate this, fig. 15 shows the stray current in the earth for a short-circuit at *1* km from sending-end.

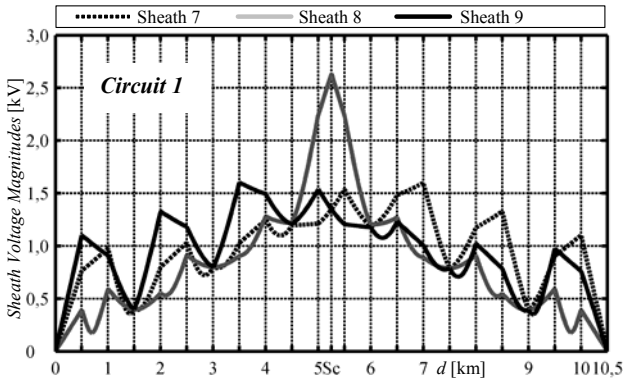

Figure 12: Circuit 1 sheath voltage magnitudes for phase 2-sheath 8 short-circuit at line midpoint

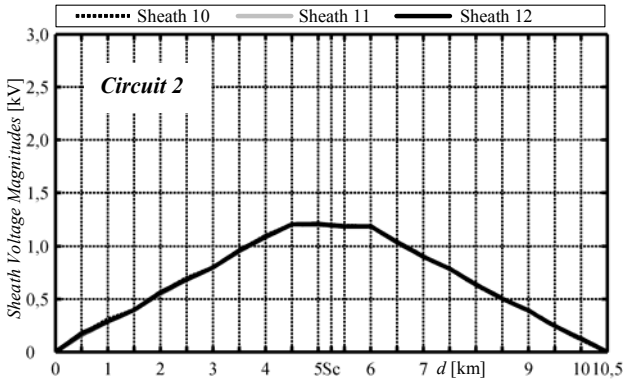

Figure 13: Circuit 2 sheath voltage magnitudes for phase 2-sheath 8 short-circuit at line midpoint

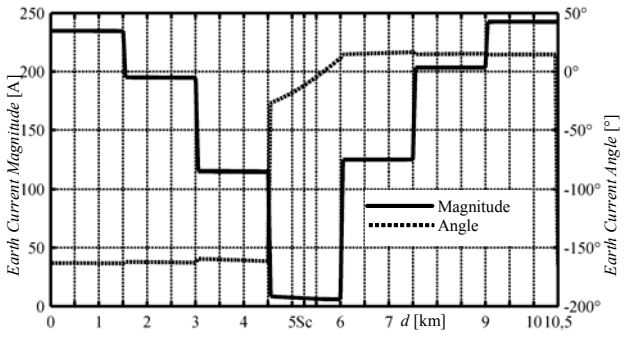

Figure 14: Stray current in the earth for phase 2-sheath 8 short-circuit at line midpoint

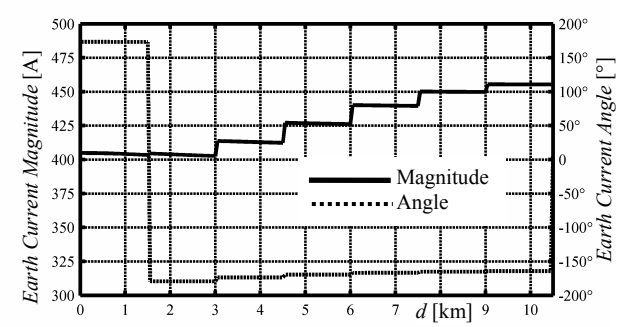

Figure 15: Stray current in the earth for phase 2-sheath 8 short-circuit at 1 km from sending-end

APPLICATION TO EHV UGC IN A TUNNEL INSTALLATION

Another important type of cable installation is inside a dedicated tunnel. Examples of this are in Germany [15], in Spain [16] etc. Both the cited systems are a double-circuit. In order to show the great flexibility of the present multiconductor procedure, the case of fig. 16 has been investigated. The data of power cables are reported in tab. 1.

With regard to the earthing techniques inside a tunnel, the use of its steel reinforcement can be foreseen if it is electrically continuous otherwise longitudinal earthing conductors can be either embedded in the floor or placed in suitable positions. Multiconductor cell analysis allows considering any earthing typology. For brevity's sake, only the magnetic behaviour of this installation is shown. The magnetic induction levels inside the tunnel (see fig. 17) are extremely high: this is obvious since the study line is very close to the cables (see fig. 16). In any case, the access to the tunnel of personnel for maintenance can be made with a lower or even switched off loading.

The multiconductor cell analysis allows a very precise computation of the magnetic field (by means of Biot-Savart's Law) because it also considers the currents in the sheaths with any bonding arrangement. This can be important when CB without phase transpositions is performed since the asymmetry of the system can give higher (not negligible) sheath currents.

Fig. 18 shows the magnetic induction levels outside the tunnel.

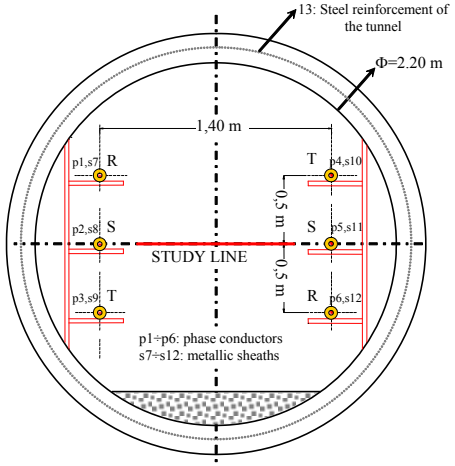

Figure 16: Double-circuit XLPE cables installed inside a tunnel

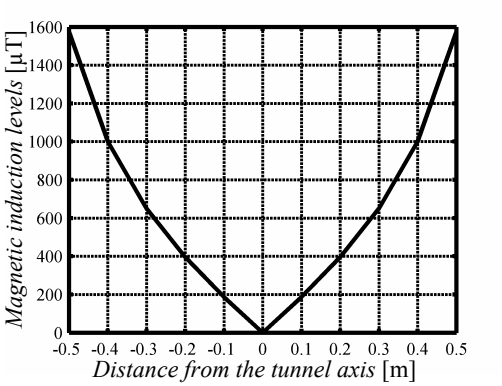

Figure 17: Magnetic induction levels inside the tunnel along the study line of fig. 16 with I=1788 A per circuit (CB with phase transpositions)

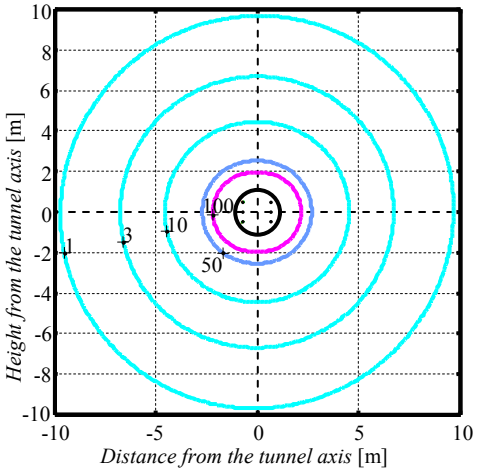

Figure 18: Magnetic induction levels outside the tunnel with I=1788 A per circuit (CB with phase transpositions)

CONCLUSIONS

The elegance and compactness of the matrix notation applied to power systems have a powerful and natural application in multiconductor cell analysis.
It allows knowing the behaviours of all the electric quantities along the line of the system conductors (including the earth) with a great detail depending on the cell length.
Accuracy of this method has been verified through some comparisons with the traditional software EMTP cable-constants routine (and finite element method as well).
The cell matrix method can assess the steady-state behaviour of any cable line: multiple circuits, SPB, SB and CB arrangements, cables installed in a tunnel considering other possible grounding conductors, mixed lines composed of the connection of an overhead line (with one or two ground wires) to a double or single-circuit UGC. Only self-made procedures demonstrate such flexibility and adaptability which are hard to find in the existing commercial software.

REFERENCES

[1] R. Benato: "*Multiconductor Analysis of Underground Power Transmission Systems: EHV AC Cables*", submitted to Electric Power Systems Research.

[2] R. Benato, M. Del Brenna, C. Di Mario, A. Lorenzoni, E. Zaccone, 2006, "A New procedure to compare the social costs of EHV-HV overhead lines and underground XLPE cables", Proc. of CIGRÉ '06, Paper B1-301.

[3] R. Benato, C. Di Mario, H. Koch, 2007, "*High capability applications of Long Gas Insulated Lines in Structures*", IEEE Trans. on Power Delivery, Vol.22, Issue 1, 619-626.

[4] R. Benato, A. Paolucci, 2005, "*Operating Capability of Long AC EHV Transmission Cables*", Electric Power Systems Research, Vol. 75/1, 17-27.

[5] R. Benato, A. Paolucci: "*Operating Capability of AC EHV Mixed Lines with Overhead and Cables Links*, accepted for publication in Electric Power Systems Research.

[6] J. R. Carson, 1926, "*Wave propagation in overhead wires with ground return*", Bell System Tech. Journal, 5, 539-554.

[7] CCITT, 1989, *Directives concerning the protection of telecommunication lines against harmful effects from electric power and electrified railway lines*. Geneva.

[8] L.M. Wedepohl, D.J. Wilcox, 1973, "*Transient analysis of underground power transmission systems*", Proc. IEE, Vol.120, N° 2, 253-260.

[9] C. Adamson, L.M. Wedepohl, 1968, "*Comparative steady-state performance of crossbonded cable systems*", Proc. of IEE, Vol. 115,No. 8, 1147-1156.

[10] R. Natarajan, T. Hunger, 2005, "*Investigations on three-phase current distribution in parallel cable conductors",* Electric Power Components and Systems, Vol. 33, N° 7, 755-766.

[11] IEC 60287-1-3, 2002, *Electric cables – Calculation of the current rating. Part 1: Current rating equations (100 % load factor) and calculation of losses. Section 3: Current sharing between parallel single-core cables and calculation of circulating current losses*.

[12] R. Benato, F. Dughiero, M. Forzan, A. Paolucci, 2002, "*Proximity Effect and Magnetic Field Calculation in GIL and in Isolated Phase Bus Ducts*", IEEE Trans. on Magnetics, Vol.38, N° 2, 781-784.

[13] ATP Rule Book, Canadian/American EMTP User Group, Portand, Oregon/USA (revised and distributed by EEUG Association, 1998).

[14] M. Kizilcay, M. Ermel, S. Demmig, H. Biewald, 1999, "*Modelling of a 400 kV XLPE cable system*", Proceedings of EEUG '99, Italy, 83-96.

[15] C.G. Henningsen, K.B. Müller, K. Polster, R.G. Schroth, 1998, "*New 400 kV XLPE long distance systems, their first application for the power supply of Berlin*", CIGRÉ '98, Paper 21-109.

[16] R. Granadino, J. Planas, M. Portillo, 2003, "*Undergrounding the first 400 kV transmission line in Spain using 2 500 mm^2 XLPE cables in a ventilated tunnel: the Madrid "Barajas" airport project*", JICABLE '03, Paper A.1.2.

GLOSSARY

UGC: UnderGround Cable
EHV: Extra High Voltage
XLPE: cross-linked polyethylene
CB: Cross-Bonding
SB: Solid-Bonding
SPB: Single-Point Bonding
EMI: Electro-Magnetic Interference